



An Inexpensive, Portable Device for Point-of-Need Generation of Silver-Nanoparticle Doped Cellulose Acetate Nanofibers for Advanced Wound Dressing

Francis Brako, Chaojie Luo,* Duncan Q. M. Craig, and Mohan Edirisinghe

This short communication describes the design and assembly of a new, miniaturized electrospinner to produce nanofibers at the site of need for drug delivery and wound dressing applications. The portable apparatus would eliminate the storage and transportation concerns with regards to the delicate nature of drug-loaded nanofibers, thereby preserving product integrity at the site of use. Furthermore, the setup features a smaller size, a cheaper price, and components that are readily obtainable off-the-shelf, compared to those of available devices that are custom-built and more expensive, making it desirable and accessible for other users in the field. As a proof-of-concept for wound care, the device is successfully used to electrospin three types of nanofibers comprised of pure cellulose acetate (CA), and CA respectively doped with 0.75 and 1.5 wt% silver nanoparticles. The miniaturized device is useful on account of the popularity of electrospinning as well as the potential to minimize wound infection due to the reduced manipulation of both the dressing and the wound from product generation to the point of need. Work is in progress to further develop the portable device and compare its product performance with traditional wound dressing materials for clinical translation.

1. Introduction

Nanofibers containing active pharmaceutical ingredients (APIs) that allow the controlled delivery of therapeutic agents ranging from proteins to antibiotics are currently attracting a great deal of interest within the drug delivery arena.^[1–3] One of the most promising applications is the treatment of wounds and burns, for which the flexibility of the macroscopic mesh structure neatly fills the lesion, while simultaneously enables high perme-

ability for exuding fluid from the wound. Furthermore, the biomimetic properties of the nanofibers may allow resemblance to the extracellular matrix and hence facilitate tissue regrowth. Tunable release of therapeutic agents such as antibiotics and growth factors is also possible by incorporation into suitable controlled release polymers, with release via diffusion and the biodegradation of the mesh itself both being attributes that may be manipulated to optimize treatment. Overall, the API-loaded nanofiber approach is highly advantageous in promoting rapid healing and minimizing infection.^[4]

Given the significant pharmaceutical potential for practical use, methods to generate highly uniform nanofibers such as electrospinning have gained widespread popularity.^[3] Electrospinning is an electrohydrodynamic (EHD) process that applies a strong electric field (kV range) to rapidly stretch a viscoelastic liquid into


micro/nanofibers. The technique is particularly attractive for its single-step, ambient condition that minimizes API degradation during processing. A broad range of materials are suitable for the process, including solutions, emulsions, gels, melts, liquid crystals, and even cells and microbes. A particular advantage of this method for drug delivery is that electrospinning produces near-monodisperse fibers and allows the precise tailoring of the size of the product without the need for templates, facilitating highly reproducible and direct encapsulation of a broad range of APIs.

On the other hand, practical healthcare applications require a formulation to be stable and unimpaired during transport and storage prior to use. Unfortunately, nanofibers are bulky following production and may be easily damaged during transportation. Generating nanofibers at the point-of-need would bypass the packaging and transportation challenges while opening a quicker route to regenerative healthcare. Valuable time to treatment would be saved as agents designed to stop bleeding, prevent infection, reduce pain, or promote healing could be administered quickly in a form which can be applied to a wide range of lesion architectures such as wounds and burns.

However, conventional electrospinning equipment is relatively large (a total size comparable to a domestic oven), heavy (weighs \approx 10 kg), with high cost ($>$ £20k), and low transportability. Recent studies have developed several purpose-built

Dr. F. Brako, Prof. D. Q. M. Craig
University College London School of Pharmacy
29-39 Brunswick Square WC1N 1AX, London, UK

Dr. C.J. Luo, Prof. M. Edirisinghe
Department of Mechanical Engineering
University College London
Torrington Place WC1E 7JE, London, UK
E-mail: chaojie.luo@ucl.ac.uk

 The ORCID identification number(s) for the author(s) of this article can be found under <https://doi.org/10.1002/mame.201700586>.

© 2018 The Authors. Published by WILEY-VCH Verlag GmbH & Co. KGaA, Weinheim. This is an open access article under the terms of the Creative Commons Attribution License, which permits use, distribution and reproduction in any medium, provided the original work is properly cited.

DOI: 10.1002/mame.201700586

apparatuses that are portable.^[4–8] While these works have significantly opened the possibility for in-field applications of nanofibers, the reported devices feature highly customized components and cannot be readily assembled using off-the-shelf sources, making the portable feature hard to access for others in the electrospinning community.

In this work, we assemble a portable electrohydrodynamic device from commercial miniature parts readily sourced off-the-shelf and demonstrate that the device is as precise and functional as conventional machines for generating nanofibers. As a proof of concept for point-of-need wound care, we use the device to electrospin three types of nanofibers comprised of pure cellulose acetate (CA), and CA loaded with 0.75 and 1.5 wt% silver nanoparticles (AgNP), respectively. An acetylated derivative of cellulose, CA is an attractive candidate for wound dressing and offers a range of advantages including hydrophilicity, nontoxicity, biodegradability, good liquid transportation and water absorption, and good solubility in common solvents allowing ready processing.^[9,10] AgNPs are loaded into the CA nanofibers for their well-known antimicrobial properties.^[11] AgNP can effectively inactivate microbes by interacting with their enzymes, proteins or DNA to inhibit microbial cell proliferation or cell division, or binding to the negatively charged bacterial cells to change the functionality of the cell membrane, thereby preventing bacterial regeneration.^[9] However, free AgNPs have external dimensions of 1–100 nm and are undesirable when used alone due to their unpredictable and potentially toxic environmental impact.^[12,13] Hence, loading AgNPs in electrospun nanofibers fixes the nanoparticles in a macroscopic structures, thereby mitigating the environmental risk while maintaining their functional advantages.^[14]

2. Experimental Section

2.1. Materials and Solution Preparation

CA (acetyl content 39.3–40.3%, average $M_w = 30\,000\text{ g mol}^{-1}$), 30–35 wt% silver nanoparticles (AgNP) dispersed in methyl triglycol, and acetone were purchased from Sigma-Aldrich (Poole, UK) and used as received. To prepare electrospun CA nanofibers containing AgNPs, CA was first dissolved in a mixed solvent of acetone: water at 4:1 weight ratio, followed by the addition and thorough mixing of an appropriate amount of AgNP dispersion. Three solution samples were prepared in which the concentration of CA was kept at 10 wt%, while the concentrations of AgNP loaded in the CA solutions were varied from 0, 0.75 and 1.5 wt%, respectively. The wt% of AgNP in CA solution was calculated based on the original AgNP dispersion in methyl triglycol at 35 wt%.

2.2. Portable Electrohydrodynamic Apparatus and Processing Conditions

The solution sample was loaded in a 10 mL syringe, attached to a commercial stainless steel, single bore needle (gauge 15) with a blunt tip. All fibers were generated using positive polarity of the voltage supply and collected using a grounded aluminum

plate. The portable electrospinning apparatus (**Figure 1**) comprised a miniature high precision microsyringe pump (Micrel mph+) and a miniature high voltage (HV) supply able to generate up to 33 kV at 10 W (EMCO 4330+). The solutions were electrospun at a positive voltage of 15 kV, a working distance of 10 cm (the distance between the needle exit and the collector), and a flow rate of 3 mL h⁻¹. All electrospinning procedures were carried out under ambient conditions (22 °C, 40–50% relative humidity, 1 atmospheric pressure).

2.3. Characterization of Solution Properties

Surface tension was measured using a Kruss Tensiometer K9 (Hamburg, Germany) by Standard Wilhelmy's plate method. Electrical conductivity was measured using Jenway 3540 pH/conductivity meter (Bibby Scientific, Staffordshire, UK). Viscosity was determined using a digital rotational viscometer, Brookfield DV-111 (Harlow, Essex, UK). All procedures were repeated five times and the mean value of the readings recorded. The calibrated equipment was cleaned with distilled water and dried before each measurement. The viscometer was calibrated automatically by following prompts to run running a complete cycle without the spindle in place. The tensiometer was calibrated by taking the surface tension of distilled water at ambient temperature. Conductivity was calibrated by immersing the probe in conductivity standard solution (Bibby Scientific, Staffordshire, UK) and the meter adjusted until a reading of 0.1194 S m⁻¹ at 22 °C was obtained.

2.4. Fiber Characterization

The surface morphology and diameter of the electrospun fibers were studied using Hitachi S-3400N scanning electron microscope (SEM). Prior to observation, each sample was coated with gold using a sputtering machine, Quorum Q150R pumped sputter coaters (Quorum Technologies, Lewes, UK) for 90 s. The average fiber diameter was determined using Image-Pro Plus software (Media Cybernetics, Inc., Rockville, MD, USA) based on at least 100 measurements from the SEM images. Thermogravimetric analysis (TGA) was carried out using Discovery TGA (TA Instruments, New Castle, USA) to assess the presence of any residue solvent as well as the water adsorption efficiency of the nanofibers as a wound-dressing candidate under physiological conditions. For characterization of water adsorption efficiency, 5 mg of the fibers was immersed in distilled water at 37 °C for 24 h, followed by gently dabbing on a soft tissue paper prior to heating. To examine the presence of AgNP in the CA nanofibers, X-ray diffraction (XRD) was carried out using D/Max-BR diffractometer (Rigaku, Tokyo, Japan) with CuK α radiation ($\lambda = 1.54\text{ \AA}$). The scanning speed was 2.0° min⁻¹ and the measurement range 2 θ was from 5° to 90° under 40 kV and 30 mA. The AgNP-loading in the CA nanofibers was quantified using localized surface plasmon resonance (LSPR) spectroscopy. The plasmon excitation wavelength for AgNP was recorded by ultraviolet-visible (UV-vis) spectroscopy (Jenway 6305 UV/Visible spectrophotometer, Bibby Scientific, Staffordshire, UK) at 430 nm after a spectrum scan of 0.01 g L⁻¹ dispersion of

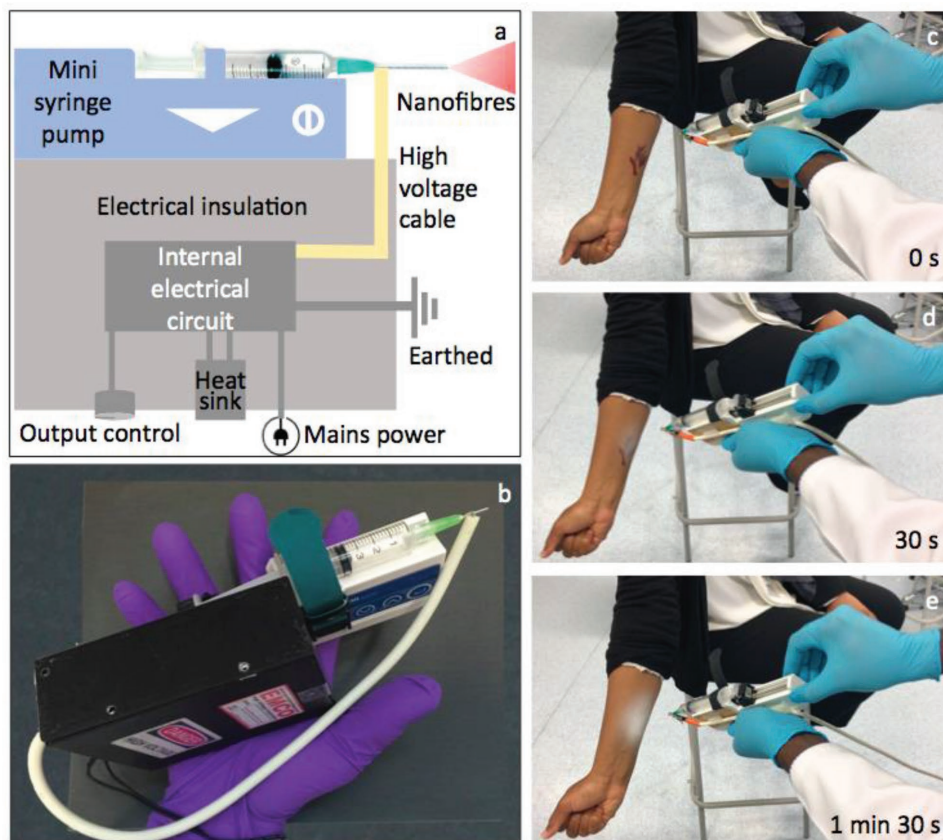


Figure 1. a) Schematic diagram of the portable EHD device. b) A photograph showing the assembly of the mini device held in hand. c–e) Snapshots of real-time recording of the operation of the mini EHD device generating nanofibers onto a mock wound in situ.

AgNP in acetone between 325 and 700 nm. Subsequently, a calibration curve was obtained by measuring absorbance of AgNP dispersions in acetone against concentrations up to 0.02 g L^{-1} , from which the AgNP content in fibers was derived. 1 mg of the CA nanofiber sample was dissolved completely in 10 mL acetone, followed by absorbance reading. Each measurement was an average of readings from three solutions. The AgNP content of the sample was then calculated based on the absorbance value on the calibration graph.

3. Results and Discussion

The components for the new portable device are simple to acquire being available off-the-shelf, featuring assembly of a high voltage (HV) supply and a precision syringe pump that are cheaper and equally as effective as the larger conventional units. The miniature HV unit, adapted from the EMCO Model R4330 series, is able to generate 0–33 kV of voltage at 10 W power, a slightly wider range than a bench-top HV supply which typically supplies 0–30 kV. The mini HV unit has a dimension of $78 \times 104 \times 35 \text{ mm}^3$, weighs 675 g, and costs £800. This is more than 95× smaller, 10× lighter, and 3× cheaper than a traditional HV unit ($\approx 7 \text{ kg}$, $200 \times 300 \times 450 \text{ mm}^3$, £2500–5000 depending on the model). The high precision mini pump from Micrel is lightweight, battery-operated and allows continuous

liquid infusion for 600 h. The liquid-crystal display, dual microcontrol motor monitors with user warning alarms, and three-digit adjustment setting allows high infusion accuracy (0.1 mL h^{-1}). Originally intended for ambulatory purposes, the pump has a compact size of $165 \times 40 \times 23 \text{ mm}^3$ at a weight of 221 g inclusive of six AAA batteries, and retails at £1000. These features make the mini pump at least 50× smaller, 10× lighter, and 2–4× cheaper than a conventional precision syringe pump for electrospinning while still providing comparable competence (e.g., Harvard Syringe Pump, UK, size: $250 \times 200 \times 150 \text{ mm}^3$, weight: 2 kg, price: £4000). Figure 1a,b shows a schematic diagram and a photograph of the complete portable assembly.

The device is simple to operate and easily handheld for direct generation of nanofibers at the point-of-need for wound care. Figure 1c–e shows snapshots of the real-time video (Supporting Information) of the device in operation on a mock wound. The apparatus was handheld at a freely adjustable angle to accurately target the wound site. The nanofibers produced adhered readily to the wound, forming a dressing on the skin without the need for any physical handling of either the nanofibers or the wound.

Prior to nanofiber fabrication, the properties of the working solutions were characterized to ensure their appropriateness for electrospinning (Table 1). Analysis of the SEM micrographs showed a slight increase in fiber diameter with increasing

Table 1. Solution properties and the as-spun fiber diameter distribution.

Solution sample	10 wt% CA	10 wt% CA + 0.75 wt% AgNP	10 wt% CA + 1.5 wt% AgNP
Conductivity [$\mu\text{S m}^{-1}$]	8.83 ± 0.07	9.24 ± 0.03	8.87 ± 0.06
Surface tension [mN m^{-1}]	27.73 ± 0.83	28.45 ± 0.03	29.20 ± 0.14
Viscosity [mPa s]	122.50 ± 2.89	130.38 ± 3.15	150.25 ± 1.71
Average fiber diameter [nm]	568 ± 141	590 ± 204	614 ± 181
Polydispersity index of fiber diameter [%]	6.14	11.9	8.68

AgNP concentration from 0 to 0.75 to 1.5 wt%. The average diameter of nanofibers electrospun from pure 10 wt% CA solution, 10 wt% CA solution with 0.75 wt% Ag, and 10 wt% CA solution with 1.5 wt% Ag were 568 ± 141 , 590 ± 204 , and 614 ± 181 nm, respectively (Figure 2 and Table 1).

Silver is a highly conductive material; it would be reasonable to expect an increase in conductivity and a decrease in fiber diameter with the increasing AgNP loading. It may hence appear counterintuitive that the conductivity of the solutions remained relatively comparable while the average fiber diameter increased with increasing AgNP. However, in this work the AgNPs added to the CA solutions were in a dispersion form rather than a pure powder. The dispersion medium methyl triglycol is a liquid with high molecular weight (164.2 g mol^{-1}) when compared to common solvents for electrospinning.^[15] Electrospinning liquids with higher molecular weight are known to produce larger fibers. The increasing quantity of the dispersion medium has also contributed to

the slight increase in viscosity as AgNP concentration in the CA solution changed from 0 to 0.75 to 1.5 wt%. Hence, the presence of methyl triglycol in the AgNP dispersion was expected to have counteracted the effect of the increasing AgNP concentration on the electrospun nanofiber diameter. Indeed, the slight increase in fiber diameter was statistically insignificant ($p = 0.05$, an Anova single factor analysis shows that $F(0.837) < F_{\text{crit}}(2.402)$) and the electrospun fiber diameter produced from the three solutions was considered to be comparable.

TGA revealed that the presence of residue solvent (acetone and water) in the pure CA nanofiber samples is minimal (dry samples listed in Table 2). On the other hand, the presence of residue solvent increased with increasing AgNP-loading concentration. Again, this is attributed to the dispersion medium of AgNP, methyl triglycol, which has low volatility (boiling point: $122 \text{ }^\circ\text{C}$), resulting in the higher presence of residue solvent in the collected fibers. The pure CA meshes showed remarkably

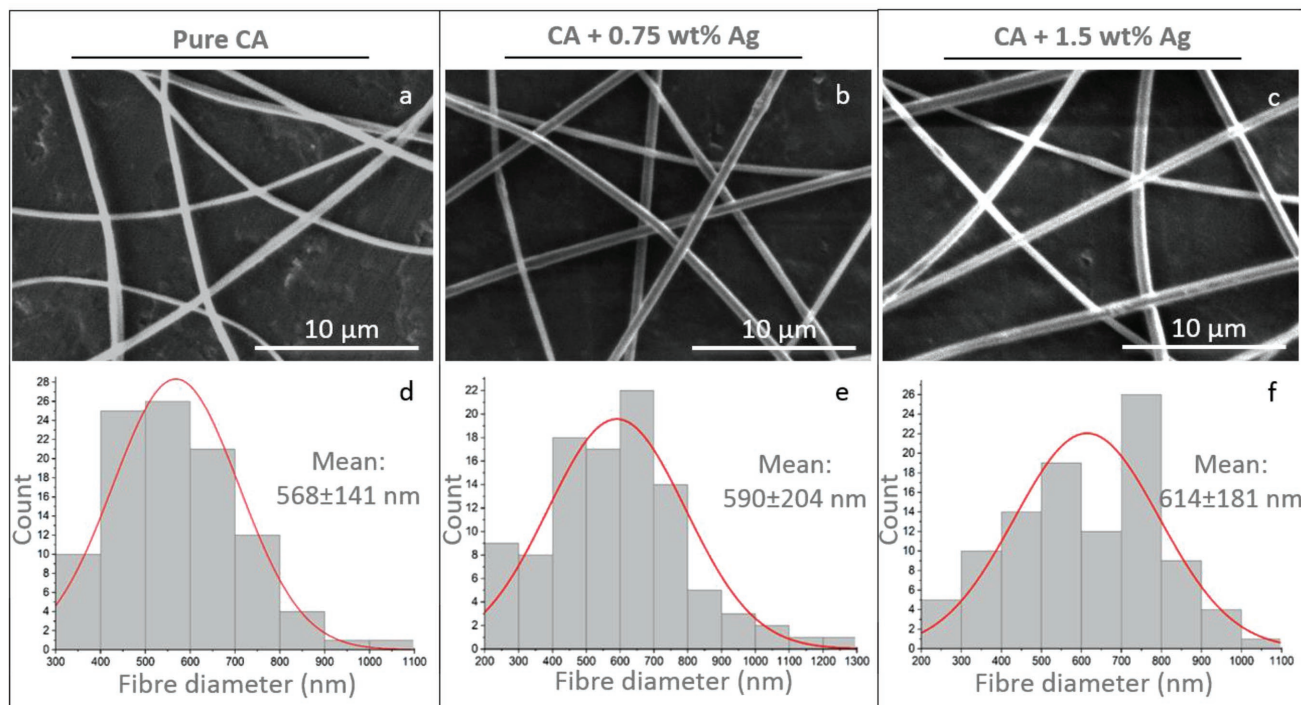


Figure 2. a–c) SEM images of CA nanofibers electrospun with various AgNP concentrations; d–f) the corresponding fiber diameter distribution profiles. Vertical left panel: pure CA nanofibers; middle panel: CA nanofibers with 0.75 wt% AgNP; right panel: CA nanofibers with 1.5 wt% AgNP. Scale bars: 10 μm .

Table 2. TGA analysis for residue solvent and water absorption capability of CA nanofiber samples.

Sample	Wt% remaining after heating	
	At 100 °C	At 200 °C
Dry 10 wt% CA	98.3	94.7
Dry 10 wt% CA + 0.75 wt% AgNP	95.5	87.0
Dry 10 wt% CA + 1.5 wt% AgNP	87.5	77.0
Soaked 10 wt% CA	50.0	50.0
Soaked 10 wt% CA + 0.75 wt% AgNP	97.7	96.8
Soaked 10 wt% CA + 1.5 wt% AgNP	98.3	97.6

better water absorption capability (soaked samples listed in Table 2) when compared to the water-immersed AgNP-loaded CA fibers. This indicates that the AgNP-loading has decreased the water absorption property of the CA meshes. Considering the importance of liquid transport and fluid absorption in wound dressing, it may be useful (though outside the scope of this work) to carry out further study to understand the antimicrobial benefit of adding AgNP in CA nanofibers versus their effect in reducing the water absorption ability of the CA nanofibers.

The presence of AgNP in the CA nanofibers was qualitatively confirmed by XRD (Figure 3a). Peaks at ≈ 38 , 46, 64, and 78 correspond to the four Bragg peaks reflecting the cubic crystal structure characteristic of Ag.^[16,17] Stronger Ag peaks were detected in samples prepared with 1.5 wt% AgNP when compared with those loaded with 0.75 wt% AgNP. UV-vis spectroscopy based on LSPR was employed to detect and quantify AgNP loading in the CA nanofibers (Figure 3b,c). LSPR is a phenomenon arising from the collective oscillations of free conduction band electrons in metallic nanoparticles. Several spectroscopic methods utilizing LSPR have been used to characterize metallic nanoparticles, with UV-vis spectroscopy considered the most straightforward.^[18] Depending on the

dispersion medium used, the UV absorption band of AgNP in a dispersion is between 410 and 450 nm.^[19] Our reference spectrum scan for pure AgNP dispersed in acetone indicated a peak intensity at a wavelength of 430 nm. The LSPR based UV-vis spectroscopy analysis indicated that CA fibers produced from solutions with 0.75 and 1.50 wt% of AgNP respectively contained 2.5 and 2.9 wt% AgNP.

4. Conclusions

This work reports a new portable electrohydrodynamic apparatus for in situ generation of nanofibers at the point-of-need. Distinct from existing portable electrosp spinners which require custom-built special components that cannot be easily obtained, all of the parts in our mini apparatus are sourced off-the-shelf and do not require any specialized customization for equipment assembly. This makes the portable setup highly accessible and applicable for other researchers and practitioners in the field. We used the portable device to successfully generate AgNP-loaded CA nanofibers for wound dressing applications and characterized the surface morphology and fiber diameter by SEM. TGA was carried out to assess the meshes' water adsorption efficiency and any presence of residue solvent. In addition, XRD and LSPR by UV-vis spectroscopy confirmed and quantified the AgNP loading in the CA nanofibers. This work opens a faster route for the practical use of nanofibers in patient-centered advanced wound care, whereby the delicate nanofibers no longer require packaging or transportation to the point of need, ensuring the drug formulation is intact upon use. Work is in progress to further develop the portable device and compare its product performance with traditional wound dressing materials for clinical translation. A further significant advantage is that the device can allow infusions of multiple liquids and enable the generation of core-shell and layered micro/nanostructures. The potential to produce at the point of need, sophisticated formulations containing controlled release of multiple active ingredients is highly desirable for drug delivery applications. This additional capability of the portable assembly is currently in development.

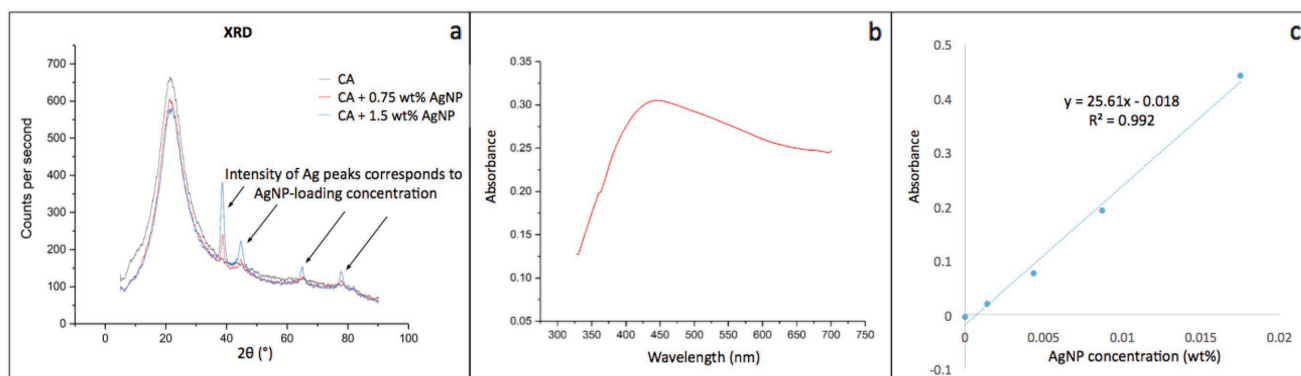


Figure 3. Qualitative and quantitative analyses of AgNP encapsulation in CA nanofibers. a) XRD patterns confirming the successful loading of AgNP in the CA fibers; the intensity of Ag peaks increased when AgNP loading increased from 0.75 to 1.5 wt%. b) UV-vis spectrum of standard 0.01 mg mL AgNP dispersed in acetone, with max wavelength at 430 nm; and c) the corresponding calibration graph from the standard AgNP dispersion in acetone.



Supporting Information

Supporting Information is available from the Wiley Online Library or from the author.

Acknowledgements

This work is funded by the Engineering and Physical Sciences Research Council, grant number EP/P022677/1.

Conflict of Interest

The authors declare no conflict of interest.

Keywords

cellulose acetate, nanofibers, portable electrospinning, silver nanoparticles, wound dressing

Received: November 17, 2017

Revised: January 22, 2018

Published online: March 24, 2018

-
- [1] J. W. Xie, X. R. Li, Y. N. Xia, *Macromol. Rapid Commun.* **2008**, *29*, 1775.
[2] P. Davoodi, F. Feng, Q. Xu, W.-C. Yan, Y. W. Tong, M. P. Srinivasan, V. K. Sharma, C.-H. Wang, *J. Controlled Release* **2015**, *205*, 70.

- [3] S. Qi, D. Craig, *Adv. Drug Delivery Rev.* **2016**, *100*, 67.
[4] P. Sofokleous, E. Stride, W. Bonfield, M. Edirisinghe, *Mater. Sci. Eng., C* **2013**, *33*, 213.
[5] W. K. Lau, P. Sofokleous, R. Day, E. Stride, M. Edirisinghe, *Bioinspired, Biomimetic Nanobiomater.* **2014**, *3*, 94.
[6] P.-A. Mouthuy, L. Groszkowski, H. Ye, *Biotechnol. Lett.* **2015**, *37*, 1107.
[7] S.-C. Xu, C.-C. Qin, M. Yu, R.-H. Dong, X. Yan, H. Zhao, W.-P. Han, H.-D. Zhang, Y.-Z. Long, *Nanoscale* **2015**, *7*, 12351.
[8] X. Yan, M. Yu, L.-H. Zhang, X.-S. Jia, J.-T. Li, X.-P. Duan, C.-C. Qin, R.-H. Dong, Y.-Z. Long, *Nanoscale* **2016**, *8*, 209.
[9] N. D. Luong, Y. Lee, J.-D. Nam, *Eur. Polym. J.* **2008**, *44*, 3116.
[10] A. Ach, *J. Macromol. Sci., Part A* **1993**, *30*, 733.
[11] W. K. Son, J. H. Youk, T. S. Lee, W. H. Park, *Macromol. Rapid Commun.* **2004**, *25*, 1632.
[12] M. Romero-Franco, H. A. Godwin, M. Bilal, Y. Cohen, *Beilstein J. Nanotechnol.* **2017**, *8*, 989.
[13] Z. Yang, Z. W. Liu, R. P. Allaker, P. Reip, J. Oxford, Z. Ahmed, G. Ren, *J. R. Soc. Interface* **2010**, *7*, S411.
[14] J. Quirós, S. Gonzalo, B. Jalvo, K. Boltos, J. A. Perdigón-Melón, R. Rosal, *Sci. Total Environ.* **2016**, *563–564*, 912.
[15] C. J. Luo, M. Nangrejo, M. Edirisinghe, *Polymer* **2010**, *51*, 1654.
[16] K. Jyoti, M. Baunthiyal, A. Singh, *J. Radiat. Res. Appl. Sci.* **2016**, *9*, 217.
[17] M. Umadevi, S. Shalini, M. R. Bindhu, *Adv. Nat. Sci.: Nanosci. Nanotechnol.* **2012**, *3*, 025008.
[18] K. A. Willets, R. P. Van Duyne, *Annu. Rev. Phys. Chem.* **2007**, *58*, 267.
[19] A. M. Abdelgawad, S. M. Hudson, O. J. Rojas, *Carbohydr. Polym.* **2014**, *100*, 166.